energies

MDPI

Article

An Energy Flow Control Algorithm of Regenerative Braking for Trams Based on Pontryagin's Minimum Principle

Ivan Župan *, Viktor Šunde, Željko Ban and Branimir Novoselnik

Faculty of Electrical Engineering and Computing, University of Zagreb, 10000 Zagreb, Croatia; viktor.sunde@fer.hr (V.Š.); zeljko.ban@fer.hr (Ž.B.); branimir.novoselnik@fer.hr (B.N.)
* Correspondence: ivan.zupan@fer.hr

Abstract: Energy savings in electric rail transport are important in order to increase energy efficiency and reduce its carbon footprint. This can be achieved by storing and using the energy generated during regenerative braking. The system described in this paper consists of a supercapacitor energy storage system (SC ESS), a bidirectional DC/DC converter, and an algorithm to control the energy flow. The proper design of the algorithm is critical for maximizing energy savings and stabilizing the power grid, and it affects the lifetime of the SC ESS. This paper presents an energy flow control algorithm based on Pontryagin's minimum principle that balances maximum energy savings with maximum SC ESS lifetime. The algorithm also performs SC ESS recharging while the rail vehicle stops on inclines to reduce the impact of its next acceleration on the power grid. To validate the algorithm, offline simulations are performed using real tram speed measurements. The results are then verified with a real-time laboratory emulation setup with HIL simulation. The tram and power grid are emulated with LiFePO4 batteries, while the SC ESS is emulated with a supercapacitor. The proposed algorithm controls a three-phase converter that enables energy exchange between the batteries and the supercapacitor. The results show that the proposed algorithm is feasible in real time and that it can be used under real operating conditions.

Keywords: regenerative braking; optimal control; supercapacitor storage system; inclination estimation; HIL simulation; Pontryagin's minimum principle

Citation: Župan, I.; Šunde, V.; Ban, Ž.; Novoselnik, B. An Energy Flow Control Algorithm of Regenerative Braking for Trams Based on Pontryagin's Minimum Principle. *Energies* **2023**, *16*, 7346. https://doi.org/10.3390/en16217346

Academic Editor: K.T. Chau

Received: 7 October 2023
Revised: 22 October 2023
Accepted: 27 October 2023
Published: 30 October 2023

1. Introduction

The constant trend of rising energy prices and harmful impacts on the environment have long put the focus on increasing energy efficiency in all electric energy consumers, especially in the transport sector. Increasing energy efficiency is also supported by EU directives such as the Energy Efficiency Directive on energy efficiency or the Commission Regulation 2019/1781 on the minimum energy efficiency of electrical motors. In electric rail transport, an increase in energy efficiency is also achieved by using energy through regenerative braking [1,2]. Savings through the use of energy generated by regenerative braking can be achieved in various ways [3] and is a globally studied problem [4]. By optimizing the timetable, regenerative braking energy can be directly exchanged between braking and accelerating vehicles on the same power grid; this type of energy exchange is suitable for metro railways where there is no influence of car traffic on the timetable. In [5], a greedy heuristic method is described for optimizing the stopping time of a rail vehicle at stations in order to exchange as much energy as possible between vehicles. Energy savings of 5.1% were achieved with this method. The paper in [6] describes the method to optimize the consumption of the power grid substation by modifying the dwell time at the station and the driving profile of the rail vehicle using Monte Carlo simulations, achieving energy savings of up to 38.6%. The use of the genetic algorithm for optimizing the departure time of rail vehicles described in the paper in [7] enables the use of an additional 4.1% of regenerative braking energy without disrupting the timetable and without affecting the

quality of passenger transport in the metro railway. A mixed-integer linear programming method was used in [8] for timetable optimization, which uses regenerative braking energy as the objective and the dwell time as the variable. The highest regenerative braking energy utilization was increased by 12.8% and the highest energy-saving rate increased by 7.39%.

In situations where regenerative braking energy cannot be used simultaneously by another vehicle on the power grid, it is preferable to store it in energy storage devices for subsequent use than to lose it irretrievably to braking resistors. Energy storage systems (ESSs) can be located outside the vehicle (stationary energy storage) or inside the vehicle (mobile energy storage). Stationary energy storage systems are usually placed near the stops of rail vehicles to minimize energy transmission losses. Since the dimensions and mass of these storage systems are not critical, they can generally store a large amount of energy. In the paper in [9], an algorithm is presented to determine the optimal position of a stationary energy storage unit to achieve maximum energy savings and voltage stabilization of the power supply system. While maintaining the existing timetable, the possibility of using up to 35% of regenerative braking energy is demonstrated. The paper in [10] shows a system with two types of energy storage devices that allow the exchange and storage of energy between two high-speed trains powered by two different power sectors, together with the compensation of unwanted distortions in the waveform of the three-phase power supply network. The result is a reduction in THD of up to 92% and a reduction in negative sequence current of almost 98%. Using the genetic algorithm in [11], the minimum of the total energy losses in the network is sought together with the minimum of the energy extracted from the feeder substations. It is shown that it is possible to use up to 93.3% of the available regenerative braking energy. In [12], the possibility of using regenerative braking energy is analyzed from the point of view of smart grids, in which stationary storage devices together with photovoltaic systems represent additional energy sources. By using mixed-integer optimization, energy savings in the range of 16% to 35% are achieved. Ref. [13] considers a smart railway station integrated with commercial buildings as an energy hub. Using a mixed-integer linear programming algorithm, the simulation results show an operation cost reduction of up to 14.2%, as well as a reduction in carbon emissions by up to 11.6% depending on the case studies. The paper in [14] considers a supercapacitor-based ESS for high-speed railway that uses a master–slave control strategy for coordinating multiple ESS controllers. This results in a reduction in energy consumption of the power substation by 8.2% using the available regenerative braking energy. An alternative use of regenerative braking energy is shown in [15], where the regenerative braking energy is used as an energy source in electric vehicle parking lots, alongside a photovoltaic energy source. The usage of regenerative braking energy significantly reduces the operational costs of electric vehicle parking lots.

Mobile ESSs are located inside or on the vehicle and eliminate the problem of energy transfer losses, but due to limited space in the vehicle, it is not always possible to install a device with the required energy capacity. The advantage of this type of device is the possibility of autonomous driving, provided the device is properly sized. The paper in [16] examines the effects of installing a mobile energy storage device in a diesel–electric train and shows the possibility of fuel savings of up to 20%. The paper in [17] presents the use of a mobile energy storage device to reduce peak current values using a genetic algorithm, resulting in a 63.49% reduction in peak current and 15.56% energy savings in substations. In [18], it is claimed that by using dynamic programming and mobile energy storage, energy savings of up to 18.23% were achieved depending on the selected weighting coefficients of the objective function. In paper [19], optimization is used to develop an algorithm that optimizes energy savings and preservation of the energy storage lifetime by minimizing the number of charge and discharge cycles. In [20], the economic viability of installing energy storage in a vehicle is also considered, along with energy savings ranging from 5.79% to 27.83%. It is shown that over a 10-year period, a profit of 73% on the initial investment can be achieved.

The ESSs used to store regenerative braking energy are usually batteries or supercapacitors (SC). Battery storage devices have higher energy density but lower power density and generally a lower number of charge and discharge cycles than supercapacitors [21]. Supercapacitors are characterized by high power density and a large number of charge and discharge cycles, but they have a lower energy density than batteries [22,23].

One of the characteristics of urban electric rail transport is frequent acceleration and braking, which suggests the possibility of frequent storage and the use of regenerative braking energy. For this type of vehicle and driving mode, SC storage devices have an advantage over batteries.

In the works in [24,25], it is found that the supercapacitor lifetime depends on temperature, in addition to voltage and current. Frequent charging and discharging of the energy storage system increases energy savings, but at the same time, the temperature also increases, which leads to a reduction in the lifetime of the ESS. It has been shown in the works in [26,27] that temperature is one of the most important factors for supercapacitor cell aging, and it has been demonstrated that supercapacitor lifetime decreases by half when the operating temperature is increased by 10 °C. For the optimal use of regenerative braking energy, it is necessary to find a compromise between maximum energy savings and minimum operating temperature of the SC ESS, taking into account the investment costs, i.e., the installed regenerative braking energy storage.

In order to increase the efficiency of the ESS, it is necessary to take into account the inclination of the vehicle route, that is, the influence of gravity, which changes the characteristics of the vehicle from the point of view of the current load on the power grid. In [28], it is shown that long distances between stations, as well as height differences between stations, lower the recuperation of regenerative braking energy. The negative influence of gravity on the energy consumption of the vehicle can be reduced by using appropriate algorithms to control the regenerative braking system [29].

The essential properties of the algorithms presented in this introduction, as well as the effect of supercapacitor temperature on its lifetime, form the basis for the development strategy of the algorithm described in this paper. The goal is to develop an algorithm that increases energy savings while taking into account the inclination of the track, but also to extend the life of the SC ESS by reducing its temperature. Extending the life of the SC ESS will allow the SC units to be replaced less frequently in a tram, increasing the economic incentive to install them. It is also possible to exert an additional stabilizing effect on the voltage of the power grid by estimating the instantaneous inclination of the track, which is especially useful in older power grids whose voltage varies significantly with higher loads.

The algorithm presented in this paper is based on Pontryagin's minimum principle. The algorithm optimizes the maximum saving of the energy extracted from the power grid and the minimization of the final temperature of the SC ESS, taking into account the inclination of the track. The result allows maximum energy savings while maintaining the maximum specified lifetime of the SC ESS. Recharging the SC during uphill driving and using this energy during the uphill drive reduces the current peaks of the power grid, resulting in a lower load on the voltage of the power grid. The description of the regenerative braking system model along with the inclination estimation method can be found in Section 2, and Pontryagin's minimum principle is presented in Section 3. In Section 4, the results of the simulation in the MATLAB programming environment are given, along with the results of the HIL simulation of the scaled model, while the conclusion is in Section 5.

2. Regenerative Braking System and Algorithm Requirements

2.1. Regenerative Braking System Requirements

This paper considers the justification of the installation of SC ESS in the TMK 2200_K tram (manufactured by Končar Elektroindustrija d.d. and TŽV Gredelj d.o.o. from Zagreb). The tram on which the supercapacitor energy storage system for regenerative braking is

installed has three drive stands, each with two 65 kW AC traction motors supplied from the power grid by a DC overhead catenary line with a nominal voltage of 600 V.

The vehicle currently uses hybrid braking, i.e., regenerative and hydraulic braking. With the existing regenerative braking system, the energy is fed back into the DC power grid without the possibility of storing it in an ESS. In situations where the voltage of the catenary rises above the maximum allowed value, the electrical energy is dissipated at the braking resistors, since this energy cannot be taken over by other vehicles on the same catenary. Sometimes a hydraulic brake is used to bring the vehicle to a stop. In the following, only regenerative braking of vehicles with the possibility of storing energy in the SC ESS is considered, since hydraulic braking is controlled by a different system.

The basic components of the proposed regenerative braking system of the vehicle are the power grid, the vehicle, the ESS, the bidirectional DC–DC converter for energy conversion between the ESS and the main drive converter of the vehicle, and the charging and discharging algorithm of the SC [30]. The energy generated by regenerative braking is stored in the SC ESS and used to start and accelerate the vehicle according to the requirements of the control algorithm. In this way, the consumption of the tram vehicle is reduced and short-term autonomous driving is enabled. During regenerative braking of the vehicle under consideration, currents of up to 1200 A occur. Due to the subsequent installation of the SC ESS in the limited available space of the vehicle body, the SC is not optimally dimensioned for the currents that occur during acceleration and braking. The available space allows a maximum SC capacity of 15.75 F and a voltage of 500 V.

2.2. Algorithm Requirements

There are three conflicting requirements for using the SC ESS to store and subsequently use tram braking energy: (i) due to increasing energy savings, the goal is to store as much braking energy as possible for subsequent use, i.e., to take as little energy as possible from the power grid; (ii) in order to preserve the lifetime of the SC ESS, the aim is to use it in such a way that it heats up as little as possible, i.e., that the temperature of the SC ESS is as low as possible; and (iii) the aim is to recharge the SC ESS when standing at a station on an uphill inclination in order to reduce as much as possible the impact on the voltage of the power grid the next time the tram starts and accelerates.

The recharging of the SC ESS according to requirement (iii) results from the characteristics of the observed power grid. Namely, a single vehicle can drop the voltage of the power grid by up to 50 V when starting and accelerating on an incline. The simultaneous acceleration of several vehicles on the same power grid sector can easily cause an interruption in the operation of the substation if the voltage of the power grid is below 420 V. There is another reason for refilling the SC ESS at the uphill station: the influence of gravity reduces the regenerative braking current by up to 50%. Recharging is carried out with a relatively low current, because the time for passenger exchange at the station is generally long enough to significantly recharge the SC ESS.

3. Regenerative Braking System Model

The representation of the simulation model of the entire system in the MATLAB/Simulink programming environment is in Figure 1. The development of the energy flow management algorithm requires a developed mathematical model of the rail vehicle, a model of the power grid, and a model of the ESS. The system model does not include a converter model because its dynamics are negligible compared with the dynamics of the energy flows.

The input to the vehicle model is the vehicle speed v, and the output is the current vehicle power p. The vehicle power is divided by the instantaneous value of the grid voltage u_l, and the result is the instantaneous vehicle current i_d, the value of which serves as input to the energy flow management algorithm. The algorithm decides the direction of the supercapacitor storage energy flow depending on the vehicle current i_d and the voltage and temperature of the supercapacitors u_{SC} and T_{SC}. The output of the block representing the algorithm is the reference current of the SC ESS $I_{\mathrm{SC\_ref}}$. The sum of the SC current

and the vehicle current is the grid current i_l, which is the input for the power grid model. The input to the supercapacitor electrothermal model is the current I_{SC_ref}, and its outputs are the instantaneous supercapacitor voltage u_{SC} and the instantaneous supercapacitor temperature T_{SC}.

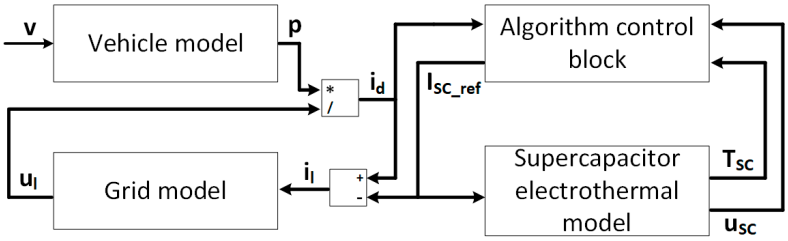

Figure 1. Regenerative braking system model with included supercapacitor electrothermal model.

3.1. Tram and Track Inclination Model

The tram and power grid simulation models in Figure 2 can be used to estimate the line inclination. The inclination is estimated by comparing the modeled tram current on a flat part of the track and the measured instantaneous current. For this purpose, the equation for the total traction force F_v is used:

$$F_v = ma + Av^2 + Bv + C + mg\sin\alpha, \tag{1}$$

where:

m—mass of the tram vehicle;
a—tram acceleration;
v—tram speed;
g—gravitational acceleration;
α—track inclination;
A, B, and C—coefficients from the Davis formula used to model the tram's friction forces [31].

Multiplying the total traction force F_v with the tram speed v results in the tram's mechanical power P_v which is equalled to the tram's electrical power:

$$F_v \cdot v = u_l \cdot i_d \,. \tag{2}$$

The only difference in mechanical power between driving on an inclined track compared with driving on a straight track is the factor $v \cdot mg \cdot \sin\alpha$. Subtracting the straight track mechanical power from the inclined track driving and equalizing the difference in electrical power results in

$$v \cdot mg\sin\alpha = u_l \cdot \Delta i_d, \tag{3}$$

where Δi_d is the current difference that compensates the effect of the track inclination on the tram electrical power. From (3), the sine of the track inclination is

$$\sin\alpha = \frac{u_l \cdot \Delta i_d}{v \cdot mg}. \tag{4}$$

The difference between the simulated vehicle current obtained from the vehicle model for a straight track and the measured vehicle current while driving can be used as a measure of the inclination of the track.

It should be noted that measurement uncertainty and model error can lead to significant deviations between the estimated inclination and the actual inclination while driving. For example, a significant error may occur when the vehicle is starting or when the vehicle is accelerating with excessive power, i.e., current. In this case, the result of the estimation according to (4) would be an inclination, even if the vehicle is on a straight part of the track. Therefore, inclination values are calculated when the vehicle has a sufficiently high driving

speed. Simulation experiments show that good inclination estimation results are obtained at speeds higher than 0.5 m/s. The simulation model created in MATLAB is shown in the block diagram in Figure 2.

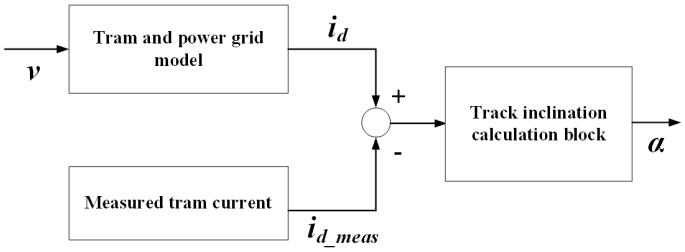

Figure 2. Simulation model of the block for estimating the inclination of the track.

The track inclination determined in the previously described way for a tram line with a steep gradient (tram line in the city of Zagreb, No. 14) is shown in Figure 3. The same figure also shows the elevation profile of the track for line No. 14, which was generated using the Google Earth application. It can be seen that there are deviations due to the measurement noise and the sensitivity of the estimation method, but also that the estimated inclination value closely follows the elevation profile of the line on which the vehicle is running.

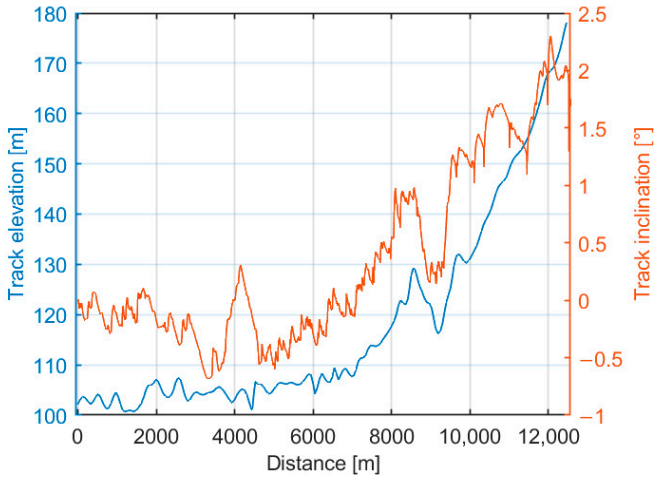

Figure 3. Track elevation for line No. 14 determined using the Google Earth application (blue) and the estimated inclination of the track for line No. 14 (orange).

The estimated inclination of the track is used during the implementation of the SC recharge algorithm in zones of higher track inclination. From Figure 3, it can be seen that a good agreement of the inclination estimate with the elevation is achieved at an estimated inclination of more than 0.5° when the tram starts to run in a zone with a significant inclination.

3.2. Power Grid Model

The power grid model consists of a series connection of an ideal DC voltage source U_G, the grid resistance R_l, and grid inductance L_l. The model input is the instantaneous power grid current i_l, and the model output is the instantaneous power grid voltage u_l:

$$u_l = U_G + i_l R_l + L_l \frac{di_l}{dt} . \quad (5)$$

The model does not take into account the influence of other vehicles in the power grid and the distance of the observed vehicle from the power grid station, which would affect the value of resistance and inductance of the catenary.

3.3. Supercapacitor Electrothermal Model

The electrothermal model of the supercapacitor consists of an electrical and a thermal model. The electrical model consists of a series connection of the capacitance C_{SC} and the resistance R_{esr}. The capacitance C_{SC} represents the total capacitance, and the resistance R_{esr} represents the total equivalent series resistance of all cells in the module. This model is used to calculate the accumulated energy in the SC ESS, the value of the voltage, and the power dissipation.

The thermal model consists of the thermal capacitance C_{th}, thermal resistance R_{th}, ambient temperature T_{amb}, and current source P_{loss}, which represents the thermal losses caused by the equivalent series resistance R_{esr}. Using the analogy between electrical and thermal quantities, the thermal resistance and capacitance are represented by electrical resistances and capacitances, as in Figure 4.

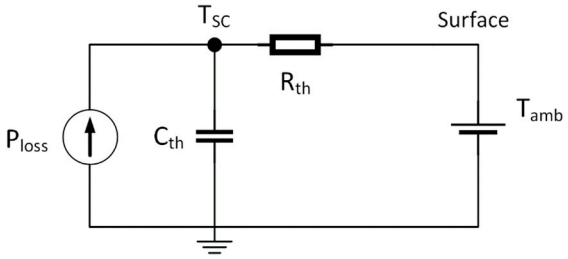

Figure 4. SC thermal model.

The electrothermal model input is the supercapacitor current i_{SC}, and the outputs are the supercapacitor voltage u_{SC} and temperature T_{SC}:

$$u_{SC} = i_{SC}R_{\text{esr}} + \frac{1}{C_{SC}}\int i_{SC}dt, \tag{6}$$

$$\dot{T}_{SC} = \frac{1}{C_{th}}\left(\frac{T_{\text{amb}} - T_{SC}}{R_{th}} + i_{SC}^2 R_{\text{esr}}\right). \tag{7}$$

4. Supercapacitor Reference Current Calculation

4.1. Supercapcacitor Reference Current Calculation during Incline Stops

Continuous estimation of the track inclination allows implementation of an algorithm to recharge the SC ESS when the tram stops at a station on an incline. Recharging in such situations has the effect of reducing the load on the power grid the next time the tram accelerates. As mentioned in Section 2, trams in the Zagreb railway can have acceleration currents of up to 1200 A, so reducing this current is essential to avoid significant voltage drops in the power grid.

The algorithm recharges the SC ESS with a current of 100 A as long as the SC ESS can be recharged if the condition that the tram is on an ascent with an estimated inclination of more than 0.5° is fulfilled. An inclination greater than 0.5° is considered a significant incline. The empirical value for the recharging current of 100 A was chosen for two reasons:

1. Given that the tram stopped by regenerative braking, it is assumed that the SC ESS already has a significant amount of energy stored; so, no excessive recharging current is required.
2. The use of excessive recharging current indirectly affects the voltage of the power grid, which negatively affects other trams running on the same grid sector. A current of 100 A causes a voltage drop in the power grid sector of fewer than 5 V, which is less than 15% of the average current load on the power grid sector from operating a tram on the observed power grid sector. By choosing such a recharging current, it is possible to recharge a larger number of vehicles at the same time without significantly stressing the power grid.

4.2. Supercapacitor Reference Current Calculation during Acceleration and Braking

Pontryagin's principle of minimum is used to calculate the (optimal) reference current of the SC ESS from the point of view of maximum energy saving and minimum operating temperature of the SC ESS [32]. The reason for using Pontryagin's principle is that in the general case, the optimal waveform of the control variables can be calculated, especially when constraints are imposed on the value of the state variables or the control variable. An additional advantage is that the system parameters can be changed so that the subsequent calculation of the optimal waveform of the control variable takes the parameter changes into account. The sudden appearance of nonmodeled features, as well as the model configuration, make the calculated optimal solution suboptimal. Moreover, when applying this principle in complex systems, it is often not possible to obtain an analytical solution, and for this reason, the principle is sometimes not suitable for online use. For this reason, the model of the regenerative braking system is simplified in this paper to facilitate the calculation of the optimal current. The power grid is modeled as an ideal power source that, together with the SC ESS, meets the vehicle's power requirements at all times. The resistance values R_{esr} in high-voltage supercapacitors are relatively small, and for simplicity, their influence on the supercapacitor voltage is ignored in the derivation of Pontryagin's minimum principle, but their influence on the temperature of the supercapacitor is taken into account, as shown in Figure 5.

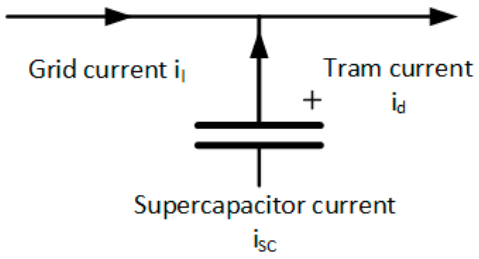

Figure 5. Energy flows in a simplified model of the regenerative braking system.

The power grid–tram–SC ESS system is described by the following equations:

$$i_d = i_l + i_{SC}, \tag{8}$$

$$u_{SC}(t) = -i_{SC}R_{\text{esr}} - \frac{1}{C_{SC}}\int_0^{t_b} i_{SC}dt \approx -\frac{1}{C_{SC}}\int_0^{t_b} i_{SC}dt, \tag{9}$$

$$\dot{u}_{SC}(t) \approx -\frac{1}{C_{SC}}i_{SC} + u_{\text{SC0}}, \tag{10}$$

$$\dot{T}_{SC}(t) = \frac{1}{C_{th}}\left(\frac{T_{\text{amb}} - T_{SC}}{R_{th}} + i_{SC}^2 R_{\text{esr}}\right), \tag{11}$$

where u_{SC0} is the supercapacitor voltage at time $t = 0$.

The previously stated conflicting requirements (maximum savings and minimum operating temperature) can be combined within the criterion function $J(i_{SC})$:

$$J(i_{SC}) = K_T T_{SC}(t_b) + \int_0^{t_b} (i_d - i_{SC})^2 dt. \tag{12}$$

where $T_{SC}(t_b)$ is the final temperature of the supercapacitor at the end of the optimization problem at time $t = t_b$, i.e., the tram acceleration process, and K_T is the penalty coefficient of the final temperature criterion. The choice of the coefficient K_T can influence the desired ratio of the influence of the criteria, the final temperature of the supercapacitor, and the minimum grid current; a smaller value of the criterion reduces the grid current, which

increases the use of the supercapacitor and thus its temperature, while a larger value of K_T has the opposite effect.

The system's Hamiltonian is described with the following equation:

$$H(T_{SC},\ u_{sc},\ i_{sc},\ \lambda_1, \lambda_2,\ t) = (i_d - i_{SC})^2 + \lambda_1 \dot{T}_{SC} + \lambda_2 \dot{u}_{SC}, \tag{13}$$

where $\lambda_1(t)$ and $\lambda_2(t)$ are the Lagrange multipliers of the Hamiltonian. The Lagrange multipliers are calculated by satisfying the following conditions:

$$\dot{\lambda}_1 = -\frac{\partial H}{\partial T_{SC}} = \frac{1}{C_{th}R_{th}}\lambda_1, \tag{14}$$

$$\dot{\lambda}_2 = -\frac{\partial H}{\partial u_{SC}} = 0, \tag{15}$$

$$\lambda_1(t_b) = \frac{\partial (K_T T_{SC}(t_b))}{\partial T_{SC}} + q_1^o = K_T + q_1^o, \tag{16}$$

$$\lambda_2(t_b) = \frac{\partial (K_T T_{SC}(t_b))}{\partial u_{sc}} + q_2^o = q_2^o. \tag{17}$$

Calculating the vector $\lambda(t) = \begin{bmatrix} \lambda_1(t) \\ \lambda_2(t) \end{bmatrix}$ is performed by solving the differential equations in (14).

The solution for $\lambda_2(t)$ is trivial:

$$\lambda_2(t) = \lambda_2(t_b) = q_2^o. \tag{18}$$

For $\lambda_1(t)$, variable separation gives the result:

$$\lambda_1(t) = C_1 e^{\frac{1}{C_{th}R_{th}}t}. \tag{19}$$

The vector $q^o = \begin{bmatrix} q_1^o & q_2^o \end{bmatrix}^T$ is the normal cone C^* of the tangent cone $C(S, x^o(t_b))$ from the set S at point $x^o(t_b)$, where $x^o(t_b) = \begin{bmatrix} T_{SC}^o(t_b) & u_{SC}^o(t_b) \end{bmatrix}^T$. The normal cone can be simply defined as the complement to the tangent cone, i.e., the set of vectors that form an angle of 90° or more with the set:

$$S = domain(T_{SC}) \times domain(u_{SC}) = [0, +\infty] \times [u_{\text{SC\_min}}, u_{\text{SC\_max}}], \text{ in } x^o(t_b) \tag{20}$$

In the case that the tangent cone is equal to $\mathbb{R}^n$, the normal cone is an empty set. In the case that $x^o(t_b)$ is on the edge of the set S, then the normal cone consists of vectors that look in the negative direction from the set S, that is, $C^* = \begin{bmatrix} q_1^o = 0 & q_2^o \end{bmatrix}^T$, where $q_1^o = 0$ because the limits $T_{SC} = 0$ or $T_{SC} = +\infty$ are never achieved, while $q_2^o < 0$ when the supercapacitor is discharged to $u_{\text{SC\_min}}$, and $q_2^o > 0$ when the supercapacitor is charged to $u_{\text{SC\_max}}$.

The optimal control variable $i_{sc}^o(t)$ must satisfy the following conditions for every t in order to fulfill Pontryagin's minimum principle:

$$H(T_{SC}^o,\ u_{SC}^o,\ i_{SC}^o,\ \lambda_1^o, \lambda_2^o,\ t) \leq H(T_{SC}^o,\ u_{SC}^o,\ i_{SC},\ \lambda_1^o, \lambda_2^o,\ t), \tag{21}$$

$$(i_d^o - i_{SC}^o)^2 + \lambda_1^o \dot{T}_{SC}^o + \lambda_2^o \dot{u}_{SC}^o \leq\ (i_d^o - i_{SC})^2 + \lambda_1^o \dot{T}_{SC}^o + \lambda_2^o \dot{u}_{SC}^o. \tag{22}$$

By writing out and subtracting the same factors from both sides, it follows that

$$-2i_d^o i_{SC}^o + {i_{SC}^o}^2 + \lambda_1^o \frac{R_{\text{esr}}}{C_{th}} {i_{SC}^o}^2 - \frac{\lambda_2^o}{C_{SC}} i_{SC}^o \leq -2i_d^o i_{SC} + {i_{SC}}^2 + \lambda_1^o \frac{R_{\text{esr}}}{C_{th}} {i_{SC}}^2 - \frac{\lambda_2^o}{C_{SC}} i_{SC}, \tag{23}$$

$$i_{SC}^{o\,2}\left(\lambda_1^o\frac{R_{\text{esr}}}{C_{th}}+1\right)+i_{SC}^o\left(-\lambda_2^o\frac{1}{C_{SC}}-2i_d^o\right)\leq i_{SC}{}^2\left(\lambda_1^o\frac{R_{\text{esr}}}{C_{th}}+1\right)+i_{SC}\left(-\lambda_2^o\frac{1}{C_{SC}}-2i_d^o\right). \tag{24}$$

It can be noticed that the result is equivalent to a parabola of the following form:

$$\gamma i_{SC}^{o\,2}+\delta i_{SC}^o, \tag{25}$$

whose minimum is trivially given by the following equation:

$$i_{\text{SC\_min}}^o=-\frac{\delta}{2\gamma}=\frac{q_2^o\frac{1}{C_{sc}}+2i_d}{2\left(1+\lambda_1^o\frac{R_{\text{esr}}}{C_{th}}\right)}, \tag{26}$$

when the following conditions are met: $\gamma>0$, $\delta<0$, so that the parabola points upward and $i_{\text{SC\_min}}$ is a positive value. Moreover, the value of $i_{\text{SC\_min}}$ must be within the interval $[-i_{\text{SC\_max}},+i_{\text{SC\_max}}]$. Therefore, the waveform of the optimal supercapacitor current has the following shape:

$$i_{SC}^o(t)=\begin{cases}\frac{q_2^o\frac{1}{C_{SC}}+2i_d}{2\left(1+\lambda_1^o\frac{R_{\text{esr}}}{C_{th}}\right)}, & \text{if } \left|i_{SC}^o(t)\right|\leq\left|i_{\text{SC\_max}}\right|,\\ i_{\text{SC\_max}}\cdot sgn(i_d), & \text{else.}\end{cases} \tag{27}$$

A more detailed description of Pontryagin's minimum principle is given in Appendix A.

5. Simulation Experiments

In order to check the validity of the developed algorithm from the previous section, an offline simulation experiment was conducted using MATLAB/Simulink and an experiment on a laboratory set-up for the emulation of SC ESS, power grids, and trams in real time (HIL simulation experiment).

5.1. Offline Simulation Experiment

The model used for the offline simulation experiment in MATLAB/Simulink is based on the mathematical models of the supercapacitor, the power grid, and tram from Section 3, as well as the control algorithm for charging and discharging the supercapacitor developed in Section 4.

The simulation includes a trip on line No. 14 of the Zagreb tram network. Line No. 14 was chosen because it has elevation differences, and more precisely, a significant rise/fall on a part of the line. The representation of the simulation model in Simulink can be found in Figure 6, while the tram speed profile used in the simulation, shown in Figure 7, was obtained from a part of the measurement of a two-day tram ride on line No. 14.

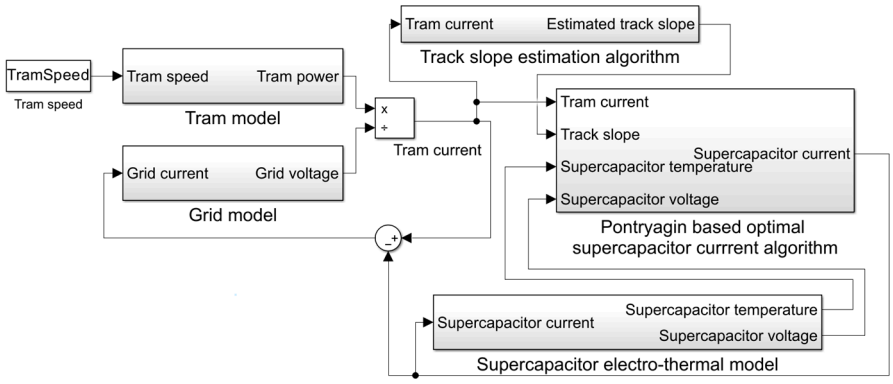

Figure 6. Simulation model of the supercapacitor, power grid, and tram system, together with the control algorithm.

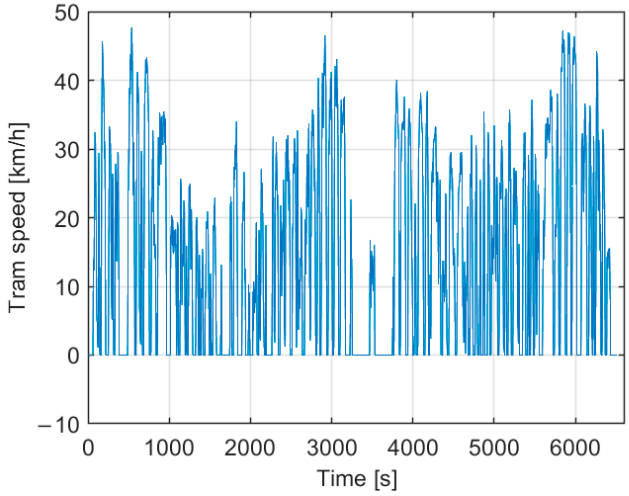

Figure 7. Tram speed profile on line No. 14 of the Zagreb tram network.

Parameters A, B, and C from Equation (1), as well as R_l, L_l, and U_G from Equation (5), were obtained by the optimization procedure described in the paper in [33]. Parameters R_{esr}, C_{SC}, R_{th}, and C_{th} in Equations (6) and (7) are obtained from the Maxwell 125 V Module BMOD0165 P125 C01 supercapacitor module catalog data.

The selection of parameters C_1, q_2^0, K_T, and K_{SC} was carried out in the following way: Empirically, the value t_b = 10 s was selected as the acceleration time of the tram. After this time, the current of the tram typically reached values of 800 A. By equalizing both criteria within the function $J(i_{sc})$, the following is obtained:

$$K_T T(t_b) = \int_0^{10} (i_d - i_{sc})^2 dt \,, \tag{28}$$

which results in K_T = 2887. Using this result in the following equation,

$$\lambda_1(t_b) = K_T = C_1 e^{\frac{1}{C_{th}R_{th}}t_b}, \tag{29}$$

the result $C_1 = 2864$ is obtained.

The value of q_2^o is calculated from the numerator of the optimum current of the SC ESS, i_{SC}^o:

$$q_2^o \frac{1}{C_{sc}} + 2i_d = 0, \tag{30}$$

where q_2^o is the minimum current of the vehicle i_d for which the optimal current i_{sc} will be equal to zero, i.e., the algorithm will determine the optimal SC current that has the same sign as the current of vehicle i_d. By choosing $i_d = 30\ A$, the result $q_2^o = 2{\cdot}30{\cdot}63 = 3780$ is obtained. The choice of $i_d = 30\ A$ is based on the fact that the SC ESS is not used in situations where the acceleration of the vehicle, i.e., the vehicle current, is very low, so as not to use the SC ESS unnecessarily.

Following the work in [30], the temperature dependence of the maximum charging current of the SC ESS is introduced. In this work, the exponential dependence of the maximum charging current on the supercapacitor temperature is used according to the following formula:

$$i_{\text{sc\_max}} = 240\, e^{\frac{65-T_{sc}}{K_{SC}}}. \tag{31}$$

The above formula is used to set a maximum charging current of 400 A at an SC temperature of 25 °C and a current of 240 A at a temperature of 65 °C. This is the maximum

operating temperature specified in the catalog at a current of 240 A. The scaling coefficient K_{SC} is selected according to the following equation to set the specified values:

$$400 = 240\, e^{\frac{65-25^{\circ}C}{K_{SC}}} = 240\, e^{\frac{40}{K_{SC}}}, \tag{32}$$

$$\ln \frac{400}{240} = \frac{40}{K_{SC}}, \tag{33}$$

$$K_{SC} = \frac{40}{\ln \frac{400}{240}} = 77.999. \tag{34}$$

Table 1 shows the values of every parameter used in the simulation.

Table 1. Simulation model parameters.

Parameter	Value	Parameter	Value
A	17.965	R_{th}	0.04 °C/W
B	34.536	C_{th}	33,000 J/°C
C	7827.249	T_{amb}	25 °C
U_G	600 V	u_{sc0}	500 V
R_l	0.0387 Ω	C_1	2864
L_l	0.0023 H	q_2^o	3780
R_{esr}	0.018 Ω	K_T	2887
C_{sc}	63 F	K_{SC}	77.999

5.1.1. Offline Simulation Experiment Results

In the following, the results of the system simulation with the implemented new algorithm (NA) using MATLAB/Simulink are presented. For comparison, the results of the simulation with a simple algorithm (SA) are also presented, which fills the SC ESS with current up to the maximum allowed and up to full every time the SC ESS is full and empties the SC ESS at each start of the tram with the current required by the tram to empty the SC ESS. The current reference value for this simple algorithm (SA) is

$$i_{\text{SC\_ref}} = \begin{cases} i_d, & \text{if } |i_d| \leq |i_{\text{SC\_max}}|, \\ i_{\text{SC\_max}} \cdot sgn(i_d), & \text{if } |i_d| > |i_{\text{SC\_max}}|. \end{cases} \tag{35}$$

Figures 8–10 show the characteristic quantities of the system during a tram ride. The arrows indicate the time intervals during which the SC ESS was recharged with constant current from the power grid while at the stop.

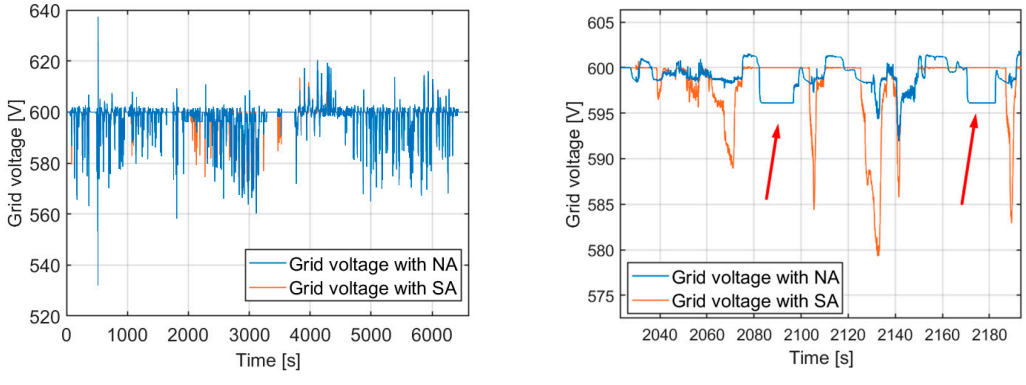

(**a**) (**b**)

Figure 8. Power grid voltage (**a**) during the entire ride, (**b**) detail during the ascent (arrows show the moments of recharging the SC).

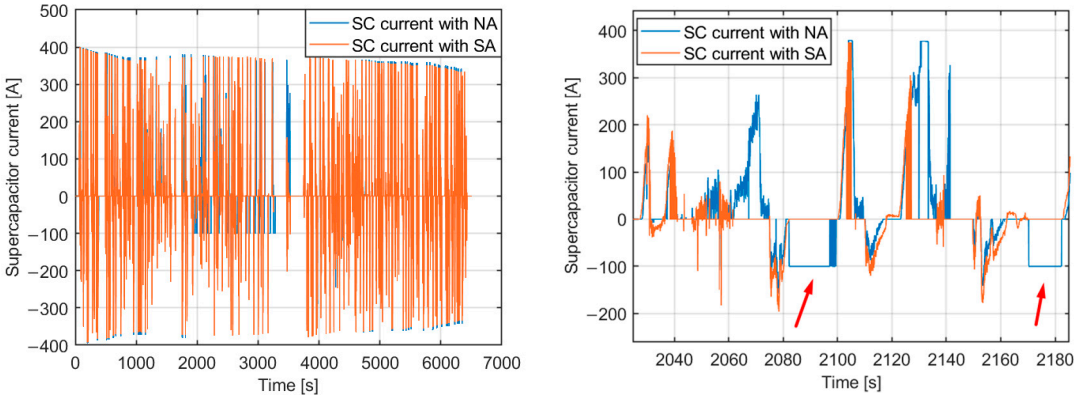

Figure 9. SC current (**a**) during the entire ride, (**b**) detail during the ascent (arrows show the moments of recharging the SC).

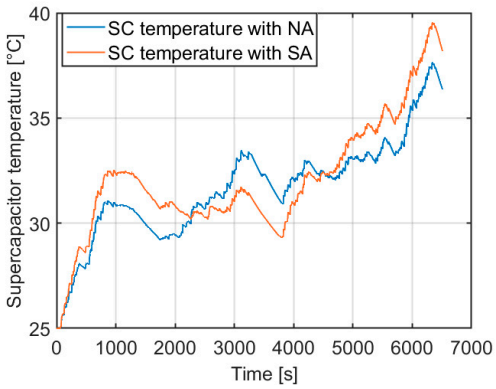

Figure 10. SC temperature waveform.

Figure 8 shows the power grid voltage waveform depending on which algorithm is used. Voltage values above 600 V indicate moments during which the tram is braking and regenerative braking energy is flowing to the power grid. Consequently, voltage values below 600 V indicate moments of tram acceleration during which energy flows from the power grid to the tram. It can be seen that the use of the NA algorithm noticeably reduces the voltage drop of the power grid, especially during the ascent, compared with the SA algorithm, meaning that the SC ESS is more frequently used. Analysis of the voltage waveform during ascent acceleration shows that the value of the average voltage during acceleration is 5.5 V lower using NA compared with SA. The reason for this is the additional energy from the SC ESS, which was stored while the tram was at the stop, which is shown with red arrows in Figure 8b. This justifies recharging the SC ESS during a stop at the tram stop in order to reduce the impact of the next acceleration on the power grid voltage.

The SC ESS current waveform is shown in Figure 9. Negative current values indicate that the SC ESS is charging, while positive values indicate discharging, which follows the energy flow from Figure 5. In Figure 9a, it can be seen that the amounts of the peak currents of the SC ESS during the incline drive are higher when the NA algorithm is used compared with the SA algorithm. The reason for this is that when the NA algorithm is used, the SC ESS can be loaded with higher current values, which depend on the temperature of the supercapacitor at that given moment. The energy available from the SC ESS is also increased when using the NA algorithm, due to the SC ESS recharging that occurs at incline stops. Figure 9b shows the difference made by recharging the SC ESS during incline stops, indicated by red arrows on the figure. It can be seen that the SC current with the SA algorithm is zero due to a lack of available energy from the SC ESS, while the recharging

from the NA algorithm allows for further SC ESS usage, reducing the impact of the tram acceleration on the power grid voltage.

Figure 10 shows the waveform of the temperature of the SC ESS. It can be seen that using the NA algorithm results in a generally lower temperature while driving on the part of the track without an incline and after the beginning of the incline. Recharging the SC ESS during stops on the incline increases its temperature, while on SA the supercapacitor is not recharged, and therefore its temperature is lower during the incline drive. The final and average values of SC ESS temperature and the amount of total stored energy from regenerative braking are given in Table 2 for the SA and NA algorithms. The table includes data for different values of the coefficient K_T for the NA algorithm to see its effect on the total stored braking energy and the temperature of the SC ESS, as well as on the operating life of the SC ESS. The effect of temperature on lifetime was performed following the work in [30], and the percentage reduction in the lifetime of the SC ESS compared with the lifetime of the SC ESS at 25 °C is given.

Table 2. Temperature values and total stored braking energy.

	Total Stored Braking Energy	Max/Average Temperature	SC Lifetime Reduction
SA algorithm	$2.984 \cdot 10^5$ J	39.5 °C/32.2 °C	40%
NA algorithm	$2.686 \cdot 10^5$ J	37.6 °C/31.77 °C	37.5%
NA algorithm (K_T·10)	$1.821 \cdot 10^5$ J	35.36 °C/30.15 °C	30%
NA algorithm (K_T/10)	$2.822 \cdot 10^5$ J	38.18 °C/32.03 °C	38.5%

From Table 2, it can be seen that the application of the NA algorithm results in lower energy savings compared with the application of the SA algorithm but in an increase in the lifetime of the supercapacitor due to the lower temperature. By changing the value of the coefficient K_T, its influence on the operation of the algorithm becomes clear: a larger value decreases the total stored braking energy but extends the life of the SC ESS due to the lower temperature, while its increase increases the total stored braking energy but generally increases the temperature of the SC ESS.

5.2. HIL Simulation Experiment

In order to experimentally verify the feasibility of the algorithm in real time, a HIL laboratory setup was created to emulate the tram–power grid–supercapacitor system, shown in Figure 11. This allowed the validity of the algorithm to be verified in real time without the need for testing in the tram, resulting in financial savings.

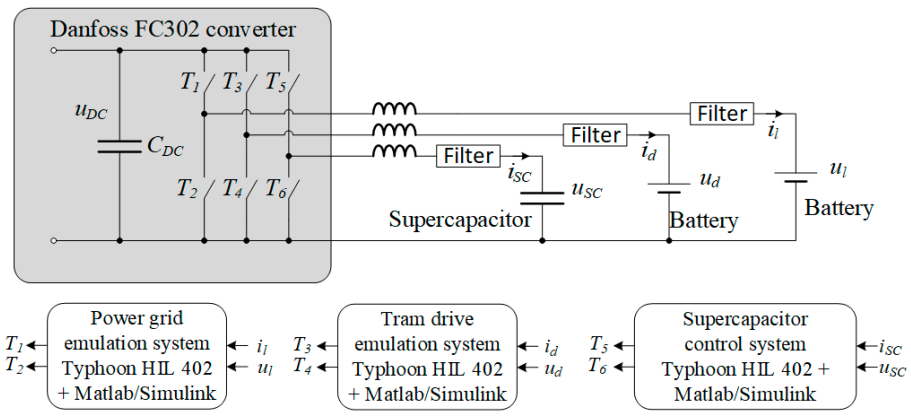

Figure 11. Structure of the HIL laboratory setup.

The mathematical models of the tram, power grid, and control system previously developed in MATLAB/Simulink are implemented in the computer system of the Typhoon

HIL402 real-time simulation software, shown in Figure 12. The calculated quantities are physically implemented using the Danfoss FC302 converter, shown in Figure 11, such that each branch of the converter (bidirectional DC/DC converter) emulates a component of the system along with the associated inductor and energy storage element. The power converter branches connected to the LiFePO4 batteries (36 V, 12 Ah) emulate the power grid and the tram vehicle. The power converter branch connected to the supercapacitor Maxwell BMOD0083 P048 B01 (48 V, 83 F) represents a bidirectional DC/DC power converter and supercapacitor energy storage. The values calculated in the Typhoon HIL simulator become the reference values based on which the switches in the branches of the Danfoss FC302 converter are controlled. Measuring the currents and voltages in the branches enables their control in real time.

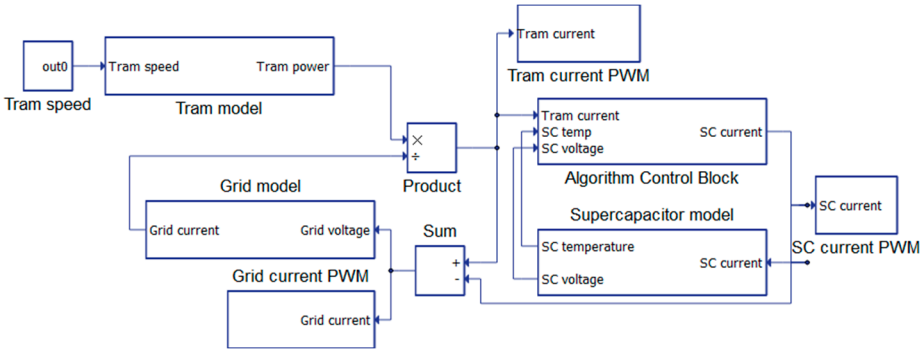

Figure 12. HIL simulation model within the Typhoon HIL programming interface.

For the purposes of the experiment, the voltage, current, and power of the real system were scaled to values corresponding to the capabilities of the LiFePO4 batteries and inverters. Due to the maximum charging current of the batteries being 4 A, the maximum currents in the converter branches were scaled from 1000 A to 4 A. Due to the oversized capacity of the batteries and supercapacitors used in the experiment, the dynamics of the voltage waveforms are too slow for effective regulation; so, in this HIL experiment, management is based only on the calculated system currents. The supercapacitor, tram, and power grid voltages are set as internal reference values for the purposes of the algorithm. The actual setup is shown in Figure 13.

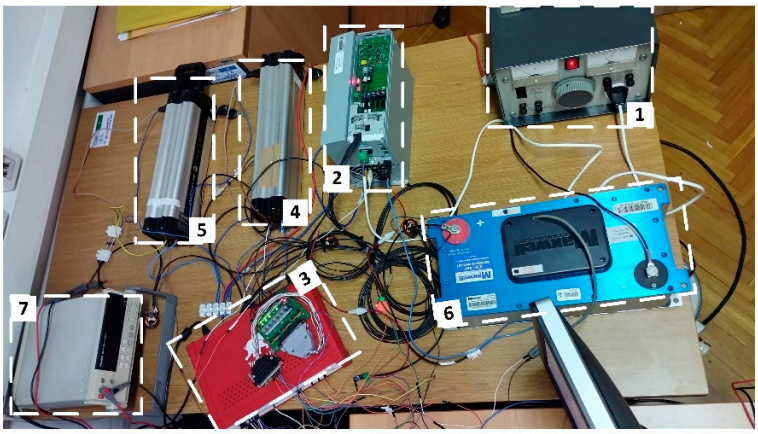

Figure 13. Laboratory setup for HIL simulation experiment: 1—autotransformer, 2—Danfoss FC302 converter, 3—Typhoon HIL402, 4, 5—LiFePO4 batteries, 6—Maxwell BMOD0083 P048 B01 supercapacitor, 7—fluke multimeter.

HIL Simulation Experiment Results

The experiment was conducted based on the speed profile presented in Section 5.1. In the laboratory model, the currents of the supercapacitor and the vehicle were measured

in real time, and the denormalized results were compared with the results of the offline simulation from Section 5.1.1. on different sections of the line (Figure 14).

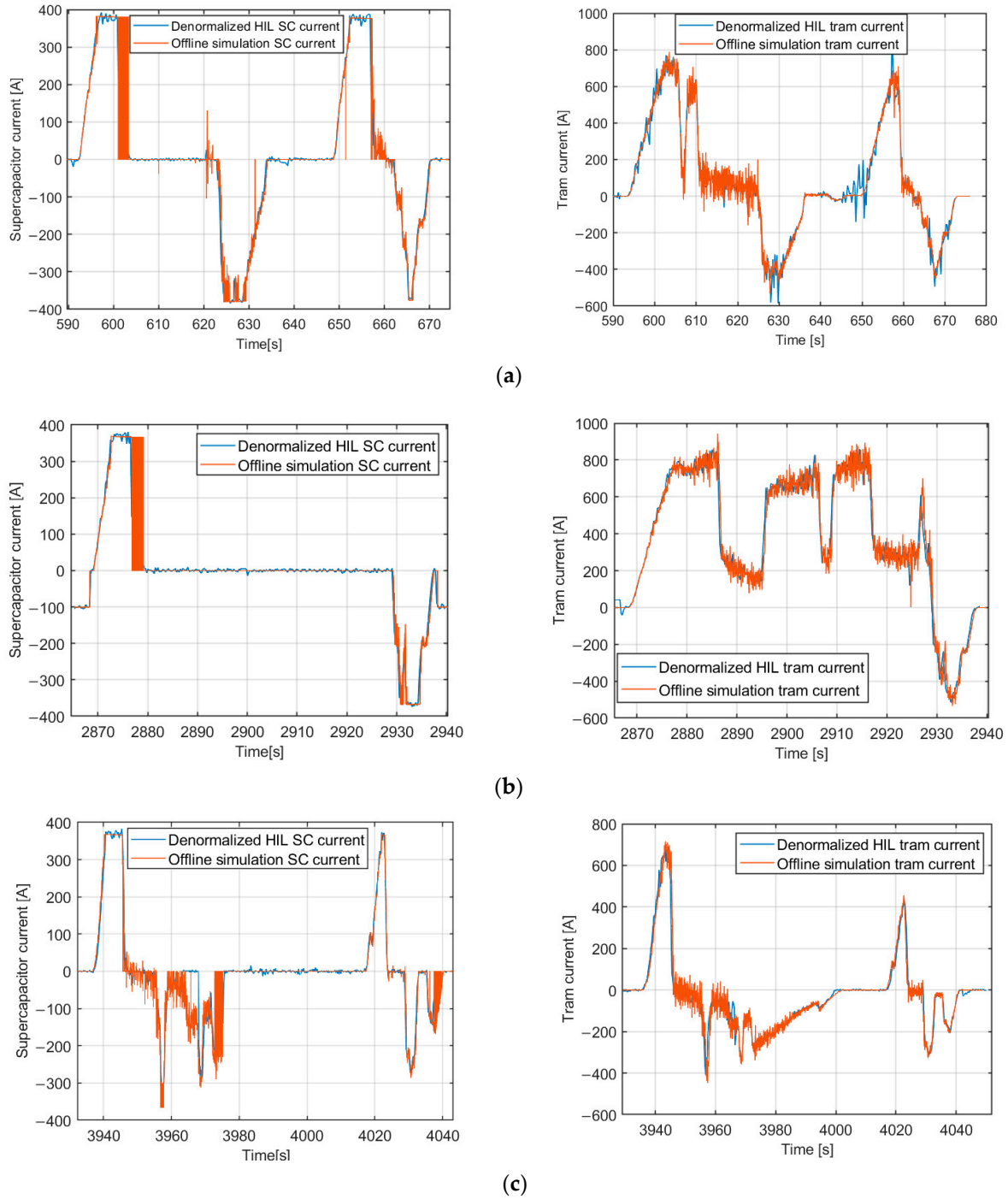

Figure 14. Denormalized currents of the supercapacitor from the HIL simulation experiment compared with the results of the offline simulation for tram driving: (**a**) on a flat part of the track, (**b**) ascent of the track, (**c**) descent of the track.

These experimental results demonstrate the feasibility of the regenerative braking energy storage system of a rail vehicle using an SC ESS with the proposed energy flow management algorithm. This provided the basis for the production of a system prototype with operating currents and voltages to be used in a rail vehicle. Moreover, the HIL simulation shows that the calculation of the optimal SC current based on Pontryagin's

minimum principle as a function of the conditions to which the tram is subjected is also possible in real time; so, high computing power is not required to implement the algorithm.

6. Conclusions

This paper describes and tests the algorithm for energy flow control in the regenerative braking system of a tram with a mobile SC ESS, which takes into account the inclination of the track and calculates the current of the SC ESS, optimizing the energy saving and the operating temperature of the SC ESS. The developed algorithm takes into account the inclination of the track so that it recharges the SC ESS while it is on an incline to compensate for a lower amount of regenerative braking current due to gravity and to reduce the increased impact of the vehicle on the power grid during its next acceleration. The inclination of the track was estimated by comparing the modeled vehicle current on the straight portion of the track with the measured vehicle current. Based on Pontryagin's minimum principle, a waveform of the reference current of the SC ESS was developed that minimizes the required current of the power grid and the operating temperature of the SC ESS. In this way, it is possible to save maximum energy and reduce the impact of the tram on the power grid, while also extending the life of the SC ESS to the maximum. The algorithm was tested by offline simulations using a model in the MATLAB/Simulink programming environment. Real-time experimental validation was performed using a Typhoon HIL device in an emulation laboratory setup. During a trip on line No. 14 of the Zagreb tram network, energy savings of $2.686 \cdot 10^5$ J were achieved. Compared with the simple algorithm for charging and discharging the SC ESS (store energy until the SC ESS is full at each brake application and extract energy from the SC ESS at each acceleration), a 10% lower energy savings was achieved, as well as a 5% lower maximum supercapacitor temperature, resulting in a 6.25% increase in the lifetime of the SC ESS. Recharging the SC ESS at stations during incline reduces the impact on the power grid voltage during acceleration by an average of 5.5 V per vehicle with an SC ESS installed, reducing the possibility of power grid interruption due to excessive load on the power grid.

The presented algorithm presents a unique perspective into combining energy savings, ESS life extension, and reduction in power grid voltage impact during incline driving within an optimal control algorithm. The ability to always have an optimal SC ESS current waveform is an advantage, but the optimality is susceptible to unmodeled uncertainties and measurement errors. The other disadvantage is the sensitivity of the incline estimation, which can cause SC ESS recharges at stops that are not on the incline and consequently negatively impact the power grid voltage. An additional feature of the proposed algorithm is the possibility to choose the emphasis of the algorithm's effect on energy savings or on the temperature of the SC ESS by choosing the desired K_T coefficient. The developed algorithm and the performed simulation experiments form the basis for the regenerative braking system which will be tested under real conditions and on a real tram vehicle. A possible future research direction is to develop a more robust inclination estimation method and increase the utilization of the installed SC as a pseudowayside ESS in moments when the SC is not used, as well as develope a coordination algorithm that will take into account a whole fleet of trams equipped with SCs.

Author Contributions: Conceptualization, I.Ž., V.Š. and Ž.B.; methodology, I.Ž. and Ž.B.; software, I.Ž.; validation, I.Ž., V.Š., Ž.B. and B.N.; investigation, I.Ž.; resources, V.Š. and Ž.B.; data curation, I.Ž.; writing—original draft preparation, I.Ž.; writing—review and editing, V.Š., Ž.B. and B.N.; visualization, I.Ž.; supervision, V.Š., Ž.B. and B.N.; project administration, V.Š. and Ž.B.; funding acquisition, V.Š. and Ž.B. All authors have read and agreed to the published version of the manuscript.

Funding: All the costs of publishing of this paper are cofinanced by the "KONTRAC GP170DC_SK" project cofunded under the Competitiveness and Cohesion Operational Program from the European Regional Development Fund.

Data Availability Statement: Data sharing is not applicable to this article. Original data was obtained from Končar—INEM within the context of the "KONTRAC GP170DC_SK" project.

Acknowledgments: The authors would like to express their gratitude to Typhoon HIL Inc. for graciously donating the Typhoon HIL402 real-time hardware-in-the-loop system and the appropriate software, as well as their technical support during the algorithm validation phase of the paper.

Conflicts of Interest: The authors declare no conflict of interest.

Nomenclature

The used nomenclature is listed by order of appearance, as follows:

ESS	Energy storage system	C_{SC}	SC capacitance
SC	Supercapacitor	R_{esr}	SC equivalent series resistance
HIL	Hardware In the Loop	C_{th}	Thermal capacitance
v	Tram speed	R_{th}	Thermal resistance
p	Tram power	T_{amb}	Ambient temperature
u_l	Grid voltage	P_{loss}	SC heat loss
i_d	Tram current	$J(\cdot)$	Criterion function
u_{SC}	SC voltage	K_T	Temperature criterion scaling coefficient
T_{SC}	SC temperature	H	Hamiltonian
$I_{\text{SC\_ref}}$	SC reference current	$(\cdot)^o$	Optimal value
i_l	Grid current	λ	Lagrange multiplier
F_v	Total traction force	q^o	Normal cone vector
m	Tram mass	C_1	Differential equation coefficient
a	Tram acceleration	C, C^*	Tangent cone, normal cone
g	Gravitational constant	S	Set
α	Track inclination	i_{SC}^o	Optimal SC current
A, B, C	Davis formula coefficient	γ, δ	Parabola coefficients
Δi_d	Tram current difference	i_{SC_min}, i_{SC_max}	Nominal minimum, maximum SC current
U_G	DC voltage source value	K_{SC}	SC current scaling coefficient
R_l	Grid resistance	NA	New algorithm
L_l	Grid inductance	SA	Simple algorithm

Appendix A Optimal Control Using Pontryagin's Minimum Principle [32]

Pontryagin's minimum (or maximum) principle is used to obtain an optimal control input for a dynamical system in order to bring it from an initial state to a final state in the presence of state and/or input constraints.

The problem of finding the optimal control according to Pontryagin is given as follows:

Find a piecewise continuous control function $u : [t_a, t_b] \rightarrow \Omega \subseteq \mathbb{R}^m$ such that the state variables $x \in \mathbb{R}^n$ are brought from an initial state $x(t_a)$ to a final state $x(t_b)$:

$$x(t_a) = x_a,$$

$$\dot{x}(t) = f(x(t),\ u(t),\ t),\ \text{for all}\ t \in [t_a, t_b]$$

$$x(t_b) \in S,$$

Such that the constraints are satisfied and the cost functional

$$J(u) = K(x(t_b),\ t_b) + \int_{t_a}^{t_b} L(x(t), u(t), t)dt,$$

is minimized.

The final time t_b can be fixed or free, i.e., it can be optimized so that the above statements are fulfilled. Furthermore, $t_a,\ x_a \in \mathbb{R}^n,\ S \subseteq \mathbb{R}^n$ are specified, and $\Omega \subseteq \mathbb{R}^m$ is a time-invariant set.

The Hamiltonian function H is an ancillary function which combines the cost functional $J(u)$ and the state equations, analogue to a Lagrangian, except that the Lagrange multipliers are functions of time. The Hamiltonian is defined as follows:

$$H(x(t),\ u(t),\ \lambda(t),\ \lambda_0,\ t) = \lambda_0 L(x(t),\ u(t),\ t) + \lambda^T(t) f(x(t),\ u(t),\ t)$$

If the control $u^o\ : [t_a,\ t_b]$ is optimal, then there exists a nontrivial Lagrange multiplier vector $\lambda(t)$

$$\begin{bmatrix} \lambda_0^0 \\ \lambda^0(t_b) \end{bmatrix} \neq 0 \in \mathbb{R}^{n+1} \text{ with } \lambda_0^o = \begin{cases} 1 \text{ in the regular case,} \\ 0 \text{ in the singular case,} \end{cases}$$

such that the following conditions are satisfied:

$$\dot{x}^o(t) = \nabla_\lambda H_{|o} = f(x^o(t),\ u^o(t),\ t),$$

$$x^o(t_a) = x_a,$$

$$\dot{\lambda}^o(t) = -\nabla_x H_{|o} = -\lambda_0^o \nabla_x L(x^o(t),\ u^o(t),\ t) - \left[\frac{\partial f}{\partial x}(x^o(t),\ u^o(t),\ t)\right]^T \lambda^o(t),$$

$$\lambda^o(t_b) = \lambda_0^o \nabla_x K(x^o(t_b),\ t_b) + q^o \text{ with } q^o \in T^*(S, x^o(t_b))^1$$

where $T^*(S, x^o(t_b))$ is the normal cone of the tangent cone $T(S, x^o(t_b))$ of S at $x^o(t_b)$.

The following condition must also be satisfied in order to prove that the control function u^o is truly the optimal control function compared with any other control function u.

For all $t \in [t_a, t_b]$, the Hamiltonian $H\left(x^o(t),\ u\ ,\ \lambda^o(t),\ \lambda_0^o,\ t\right)$ has a global minimum with respect to $u \in \Omega$ in $u = u^o(t)$:

$$H(x^o(t),\ u^o(t),\ \lambda^o(t),\ \lambda_0^o, t) \leq H(x^o(t),\ u,\ \lambda^o(t),\ \lambda_0^o,\ t)$$

for all $u \in \Omega$ and all $t \in [t_a, t_b]$.

References

1. González-Gil, A.; Palacin, R.; Batty, P. Sustainable urban rail systems: Strategies and technologies for optimal management of regenerative braking energy. *Energy Convers. Manag.* **2013**, *75*, 374–388. [CrossRef]
2. Hamada, A.T.; Orhan, M.F. An overview of regenerative braking systems. *J. Energy Storage* **2022**, *52*, 105033. [CrossRef]
3. Xing, L.; Li, X. Review of Regenerative Braking Energy Storage and Utilization Technology in Urban Rail Transit. In *The Proceedings of the 9th Frontier Academic Forum of Electrical Engineering*; Ma, W., Rong, M., Liu, W., Wang, S., Li, G., Eds.; Springer: Singapore, 2021; Volume 742, pp. 775–783.
4. Belay Kebede, A.; Worku, G.B. A research on regenerative braking energy recovery: A case of Addis Ababa light rail transit. *eTransportation* **2021**, *8*, 100117. [CrossRef]
5. Fournier, D.; Fages, F.; Mulard, D. *A Greedy Heuristic for Optimizing Metro Regenerative Energy Usage*; Civil-Comp Press: Stirlingshire, UK. [CrossRef]
6. Tian, Z.; Weston, P.; Zhao, N.; Hillmansen, S.; Roberts, C.; Chen, L. System energy optimisation strategies for metros with regeneration. *Transp. Res. Part C Emerg. Technol.* **2017**, *75*, 120–135. [CrossRef]
7. Zhao, N.; Tian, Z.; Hillmansen, S.; Chen, L.; Roberts, C.; Gao, S. Timetable Optimization and Trial Test for Regenerative Braking Energy Utilization in Rapid Transit Systems. *Energies* **2022**, *15*, 4879. [CrossRef]
8. Sun, P.; Zhang, C.; Jin, B.; Wang, Q.; Geng, H. Timetable optimization for maximization of regenerative braking energy utilization in traction network of urban rail transit. *Comput. Ind. Eng.* **2023**, *183*, 109448. [CrossRef]
9. Cipolletta, G.; Delle Femine, A.; Gallo, D.; Luiso, M.; Landi, C. Design of a Stationary Energy Recovery System in Rail Transport. *Energies* **2021**, *14*, 2560. [CrossRef]
10. Zhao, S.; Feng, Q.; Yang, H.; Zhang, Y. Control strategy of hybrid energy storage in regenerative braking energy of high-speed railway. *Energy Rep.* **2022**, *8*, 1330–1338. [CrossRef]
11. Che, C.; Wang, Y.; Lu, Q.; Peng, J.; Liu, X.; Chen, Y.; He, B. An effective utilization scheme for regenerative braking energy based on power regulation with a genetic algorithm. *IET Power Electron.* **2022**, *15*, 1392–1408. [CrossRef]

12. Sengor, I.; Kilickiran, H.C.; Akdemir, H.; Kekezoglu, B.; Erdinc, O.; Catalao, J.P.S. Energy Management of a Smart Railway Station Considering Regenerative Braking and Stochastic Behaviour of ESS and PV Generation. *IEEE Trans. Sustain. Energy* **2018**, *9*, 1041–1050. [CrossRef]
13. Akbari, S.; Fazel, S.S.; Jadid, S. Optimal operation of a smart railway station based on a multi-energy hub structure considering environmental perspective and regenerative braking utilization. *Energy Sci. Eng.* **2021**, *9*, 1614–1631. [CrossRef]
14. Chen, J.; Hu, H.; Ge, Y.; Wang, K.; Huang, W.; He, Z. An Energy Storage System for Recycling Regenerative Braking Energy in High-Speed Railway. *IEEE Trans. Power Deliv.* **2021**, *36*, 320–330. [CrossRef]
15. Cicek, A.; Şengör, I.; Guner, S.; Karakus, F.; Erenoglu, A.K.; Erdinc, O.; Shafie-Khah, M.; Catalao, J.P.S. Integrated Rail System and EV Parking Lot Operation With Regenerative Braking Energy, Energy Storage System and PV Availability. *IEEE Trans. Smart Grid* **2022**, *13*, 3049–3058. [CrossRef]
16. Cutrignelli, F.; Saponaro, G.; Stefanizzi, M.; Torresi, M.; Camporeale, S.M. Study of the Effects of Regenerative Braking System on a Hybrid Diagnostic Train. *Energies* **2023**, *16*, 874. [CrossRef]
17. Sumpavakup, C.; Ratniyomchai, T.; Kulworawanichpong, T. Optimal energy saving in DC railway system with on-board energy storage system by using peak demand cutting strategy. *J. Mod. Transp.* **2017**, *25*, 223–235. [CrossRef]
18. Liu, W.; Xu, J.; Tang, J. Study on control strategy of urban rail train with on-board regenerative braking energy storage system. In Proceedings of the IECON 2017-43rd Annual Conference of the IEEE Industrial Electronics Society, Beijing, China, 29 October–1 November 2017; IEEE: Piscataway, NJ, USA, 2017; pp. 3924–3929. [CrossRef]
19. Pavlović, T.; Župan, I.; Šunde, V.; Ban, Ž. HIL Simulation of a Tram Regenerative Braking System. *Electronics* **2021**, *10*, 1379. [CrossRef]
20. Radu, P.; Szelag, A.; Steczek, M. On-Board Energy Storage Devices with Supercapacitors for Metro Trains—Case Study Analysis of Application Effectiveness. *Energies* **2019**, *12*, 1291. [CrossRef]
21. Liu, X.; Li, K. Energy storage devices in electrified railway systems: A review. *Transp. Saf. Environ.* **2020**, *2*, 183–201. [CrossRef]
22. Zhao, J.; Burke, A.F. Review on supercapacitors: Technologies and performance evaluation. *J. Energy Chem.* **2021**, *59*, 276–291. [CrossRef]
23. Yassine, M.; Fabris, D. Performance of Commercially Available Supercapacitors. *Energies* **2017**, *10*, 1340. [CrossRef]
24. Zheng, F.; Li, Y.; Wang, X. Study on effects of applied current and voltage on the ageing of supercapacitors. *Electrochim. Acta* **2018**, *276*, 343–351. [CrossRef]
25. Kreczanik, P.; Venet, P.; Hijazi, A.; Clerc, G. Study of Supercapacitor Aging and Lifetime Estimation according to Voltage, Temperature, and RMS Current. *IEEE Trans. Ind. Electron.* **2014**, *61*, 4895–4902. [CrossRef]
26. Negroiu, R.; Ionescu, C.; Svasta, P.; Vasile, A. Influence of temperature on supercapacitors behavior in series/parallel connections. In Proceedings of the 2017 IEEE 23rd International Symposium for Design and Technology in Electronic Packaging (SIITME), Constanta, Romania, 26–29 October 2017; IEEE: Piscataway, NJ, USA, 2017; pp. 367–370. [CrossRef]
27. Reichbach, N.; Mellincovsky, M.; Peretz, M.M.; Kuperman, A. Long-Term Wide-Temperature Supercapacitor Ragone Plot Based on Manufacturer Datasheet. *IEEE Trans. Energy Convers.* **2016**, *31*, 404–406. [CrossRef]
28. Hoo, D.S.; Chua, K.H.; Hau, L.C.; Chong, K.Y.; Lim, Y.S.; Chua, X.R.; Wang, L. An Investigation on Recuperation of Regenerative Braking Energy in DC Railway Electrification System. In Proceedings of the 2022 IEEE International Conference in Power Engineering Application (ICPEA), Shah Alam, Malaysia, 7–8 March 2022; IEEE: Piscataway, NJ, USA, 2022; pp. 1–6. [CrossRef]
29. Zhang, Q.; Zhang, Y.; Huang, K.; Tasiu, I.A.; Lu, B.; Meng, X.; Liu, Z.; Sun, W. Modeling of Regenerative Braking Energy for Electric Multiple Units Passing Long Downhill Section. *IEEE Trans. Transp. Electrific.* **2022**, *8*, 3742–3758. [CrossRef]
30. Župan, I.; Šunde, V.; Ban, Ž.; Krušelj, D. Algorithm with temperature-dependent maximum charging current of a supercapacitor module in a tram regenerative braking system. *J. Energy Storage* **2021**, *36*, 102378. [CrossRef]
31. Sengor, I.; Kilickiran, H.C.; Akdemir, H.; Kilic, B. Determination of Potential Regenerative Braking Energy in Railway Systems: A Case Study for Istanbul M1A Light Metro Line. *JOACE* **2017**, *5*, 21–25. [CrossRef]
32. Geering, H.P. *Optimal Control with Engineering Applications*; Springer: Berlin/Heidelberg, Germany, 2007. [CrossRef]
33. Župan, I.; Lelas, M.; Ban, Ž.; Šunde, V. Optimizing braking energy flow through charging status surface expansion. *Eng. Rev.* **2020**, *41*, 129–140. [CrossRef]